

Monte Carlo simulations of spin glasses at low temperatures: Effects of free boundary conditions

Helmut G. Katzgraber* and A. P. Young†

Department of Physics, University of California, Santa Cruz, California 95064

(Dated: October 27, 2018)

We present results of Monte Carlo simulations, using parallel tempering, on the three- and four-dimensional Edwards-Anderson Ising spin glass with Gaussian couplings at low temperatures with free boundary conditions. Our results suggest that the surface of large-scale low-energy excitations may be space filling. The data implies that the energy of these excitations increases with increasing system size for small systems, but we see evidence in three dimensions, where we have a greater range of sizes, for a crossover to a regime where the energy is independent of system size, in accordance with replica symmetry breaking.

PACS numbers: 75.50.Lk, 75.40.Mg, 05.50.+q

I. INTRODUCTION

Recently there have been several studies^{1,2,3,4,5,6,7} that attempt to better understand the nature of the spin-glass state through zero-temperature calculations. Whereas these calculations have used different versions of the *heuristic* genetic algorithm, recently the *exact* branch and cut algorithm has been applied⁸ to the Edwards-Anderson Ising spin glass with *free* boundary conditions. In part, this choice of boundary conditions has been motivated by the algorithm being more efficient for free than periodic boundary conditions. However, in addition, use of a different boundary condition also allows one to study the role that boundary conditions play, and perhaps eventually to deduce the optimal choice of boundary conditions for numerical studies.

There have been two principle scenarios proposed for the spin-glass state. In replica symmetry breaking (RSB)^{9,10} large-scale low-energy excitations of the system cost a finite energy in the thermodynamic limit and have a surface that is space filling, i.e. the fractal dimension of the surface, d_s , is equal to the space dimension d . In the other commonly discussed scenario, called the droplet picture (DP),^{11,12,13} it is argued that the lowest-energy excitation with linear spatial extent L and involving a given spin typically costs an energy L^θ , where θ is a (positive) exponent. Hence, in the thermodynamic limit, these excitations cost an infinite energy. In addition, it is predicted that the surface of these excitations is fractal with $d_s < d$.

An intermediate picture between RSB and the DP has also been proposed by Krzakala and Martin² and Palassini and Young³ (KMPY) on the basis of numerical calculations at $T = 0$ (see also Ref. 14 for analogous calculations at finite- T). In this scenario, large-scale low-energy excitations cost a finite energy in the thermodynamic limit but their surface is fractal. There are two exponents^{2,3} that describe the energy dependence of the system size: θ (> 0), where L^θ is the typical change in energy when the boundary conditions are changed, as originally proposed by the droplet model, and θ' , where

$L^{\theta'}$ characterizes the energy of system-size excitations thermally excited within the system for a *fixed* set of boundary conditions.

The data of Refs. 2 and 3 for periodic boundary conditions agree well with the KMPY scenario, while agreement with RSB would require large corrections to scaling. However, the results of Ref. 8 appear to be somewhat different. They are compatible with RSB but it cannot be excluded that this is a finite-size effect due to large corrections with free boundary conditions, so the KMPY or droplet pictures cannot be ruled out.

In this work we perform finite temperature Monte Carlo simulations of the three- and four-dimensional Edwards-Anderson (EA) Ising spin glass with free boundary conditions at finite but low temperatures. We find results that are consistent with the ground-state calculations of Ref. 8.

To investigate differences between the models mentioned it is useful to look at the distribution of the spin overlap,^{15,16,17,18} $P(q)$. In the droplet picture,^{19,20,21} $P(q)$ is trivial in the thermodynamic limit, i.e., there are only two peaks at $\pm q_{\text{EA}}$ (q_{EA} is the Edwards-Anderson order parameter). For finite systems of linear size L , there is a tail with weight $\sim L^{-\theta}$ down to $q = 0$. Conversely, RSB predicts a tail with a finite weight down to $q = 0$ independent of system size. In addition, the variance of the distribution of the link overlap q_l (introduced below) can shed some light on the surface of the excitations: the droplet picture predicts that the variance of the link overlap has a power-law decay $\text{Var}(q_l) \sim L^{-\mu_l}$, where¹⁴ $\mu_l = \theta' + 2(d - d_s)$. Because RSB predicts that the surface of the low-energy excitations is space-filling and, in addition, that system-size excitations cost only a finite energy, one expects that $\text{Var}(q_l) \rightarrow \text{const}$ for $L \rightarrow \infty$.

The layout of the paper is as follows: In Sec. II, we describe the model as well as the observables measured, while in Sec. III, we discuss our equilibration tests for the parallel tempering Monte Carlo method. Our results are presented in Sec. IV and the conclusions summarized in Sec. V.

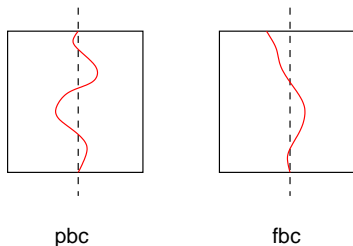


FIG. 1: Sketch of the effect of different boundary conditions on domain walls. For simplicity, we show a sample in two dimensions. The solid line with curvature represents a domain wall. Periodic boundary conditions (pbc) restrict the domain wall to enter and exit the sample at corresponding points on the top and bottom surfaces. This is not the case for free boundary conditions (fbc) where the domain wall can enter and exit the sample at arbitrary points.

II. MODEL AND OBSERVABLES

The Hamiltonian of the Edwards-Anderson Ising spin glass is given by

$$\mathcal{H} = - \sum_{\langle i,j \rangle} J_{ij} S_i S_j, \quad (1)$$

where the sites i lie on a hypercubic lattice in dimension $d = 3$ or 4 with $N = L^d$ sites [$L \leq 8$ in three dimensions (3D), $L \leq 5$ in four dimensions (4D)], $S_i = \pm 1$, and the J_{ij} are the nearest-neighbor interactions chosen according to a Gaussian distribution with zero mean and standard deviation unity. Free boundary conditions are applied. Applying free boundary conditions has the advantage that domain walls are not restricted to enter and exit the sample at the corresponding point on opposite sides of the system, as sketched in Fig. 1.

Our attention focuses primarily on two quantities: the spin overlap q , defined by

$$q = \frac{1}{N} \sum_{i=1}^N S_i^{(1)} S_i^{(2)}, \quad (2)$$

where “(1)” and “(2)” refer to two copies (replicas) of the system with identical bonds, and the link overlap, q_l , defined by

$$q_l = \frac{1}{N_b} \sum_{\langle i,j \rangle} S_i^{(1)} S_j^{(2)} S_i^{(2)} S_j^{(2)}. \quad (3)$$

In the last equation, $N_b = dL^{d-1}(L-1)$ is the number of bonds, and the sum is over all pairs of spins i and j connected by bonds.

If two spin configurations differ by flipping a large cluster then q differs from unity by an amount proportional to the *volume* of the cluster while q_l differs from unity by an amount proportional to the *surface* of the cluster.

III. EQUILIBRATION

For the simulations, we use the parallel tempering Monte Carlo method^{22,23} as it allows us to study larger systems at lower temperatures. We test equilibration with the method introduced by Katzgraber *et al.* in Ref. 14 for short-range spin glasses with a Gaussian distribution of exchange interactions. It depends on an expression that relates the average energy per spin $|U|$ to the average link overlap:

$$[\langle q_l \rangle]_{\text{av}} = 1 - \frac{T|U|N}{N_b}, \quad (4)$$

where $[\dots]_{\text{av}}$ denotes an average over samples, and $\langle \dots \rangle$ denotes a thermal average.

We choose a set of temperatures $T_i, i = 1, 2, \dots, N_T$, so that the acceptance ratios for the global moves are satisfactory, typically greater than 0.3 for $d = 3, 4$. The simulation is started with randomly chosen spins so that all replicas are uncorrelated. This has the effect that both sides of Eq. (4) are approached from opposite directions. Once they agree, the system is in equilibrium, as can be seen in Fig. 2 for $T = 0.2$, the lowest temperature simulated, with $L = 4, d = 3$. We show data for a smaller size as it allows us to generate more samples for longer equilibration times to better illustrate the method. For larger system sizes, we stop the simulation once the data for $[\langle q_l \rangle]_{\text{av}}$ and $1 - T|U|N/N_b$ agree.

In order to calculate the spin and link overlaps in Eqs. (2) and (3) we use two replicas for each temperature, and so the total number of replicas in the simulations is $2N_T$.

IV. RESULTS

A. Three dimensions

In Table I, we show N_{samp} , the number of samples, N_{sweep} , the total number of sweeps performed by each set of spins (replicas), and N_T , the number of temperature values, used in the simulations. For all sizes the largest temperature is 2.0 and the lowest 0.20 (to be compared with $T_c \simeq 0.95$).²⁴ The temperatures are chosen in order for the acceptance ratios of the global moves to be typically bigger than 0.3 for the largest size of $L = 8$.

Figures 3 and 4 show data for the spin overlap distribution $P(q)$ for temperatures 0.20 and 0.50 respectively. For low enough temperatures, our data are consistent with $P(0) \propto T$. There is a large peak for large values of q and a tail that depends slightly on the system size. To determine more precisely the size dependence of $P(0)$, we average over data points with $|q| < q_0$, where $q_0 = 0.20$. Different values for q_0 give comparable results within error bars. The results are shown in Fig. 5. Since the droplet model predicts that $P(0)$ should vary as $L^{-\theta}$, and the value of θ obtained in numerical studies involving boundary condition changes^{25,26,27} is about 0.20, we

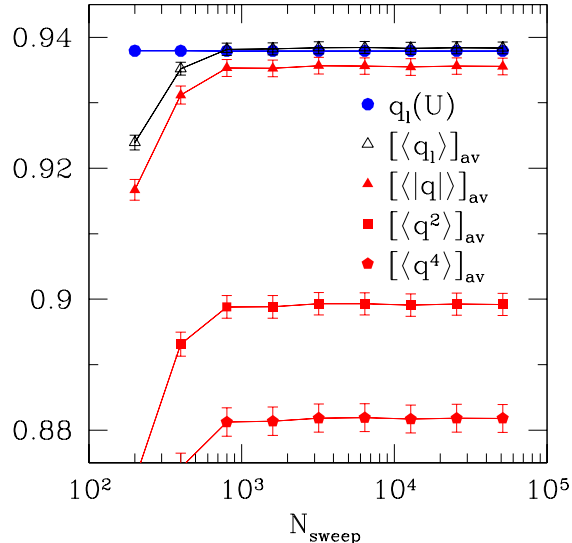


FIG. 2: The average link overlap $[\langle q_l \rangle]_{\text{av}}$, and $q_l(U)$ [the right-hand side of Eq. (4)], as a function of the number of Monte Carlo sweeps, N_{sweep} , which each of the replicas perform for $d = 3$, $T = 0.2$, and $L = 4$. Thermal averaging was performed over the last half of the sweeps indicated. The two sets of data approach each other from opposite directions and then do not appear to change at larger number of sweeps, indicating that they have equilibrated. We also show data for the average first, second and fourth moments of q . They appear to be independent of the number of sweeps once the data for q_l has equilibrated.

TABLE I: Parameters of the simulations in three dimensions with free boundary conditions. N_{samp} is the number of samples (i.e., sets of bonds), N_{sweep} is the total number of sweeps simulated for each of the $2N_T$ replicas for a single sample, and N_T is the number of temperatures used in the parallel tempering method.

L	N_{samp}	N_{sweep}	N_T
3	20000	1.0×10^4	18
4	20000	1.0×10^4	18
5	10000	1.6×10^5	18
6	10000	3.0×10^5	18
7	5000	1.0×10^6	18
8	5000	1.0×10^6	18
9	5000	3.0×10^6	18

indicate, by the dashed line in Fig. 5, a slope of -0.20 . For low temperatures and small sizes the data are compatible with this droplet theory prediction. However, we see evidence for crossover to a behavior where $P(0)$ is independent of L at larger system sizes, which would be consistent with RSB.

Fitting the data in Fig. 5 to the form $aL^{-\theta'}$ for $L \leq 7$,

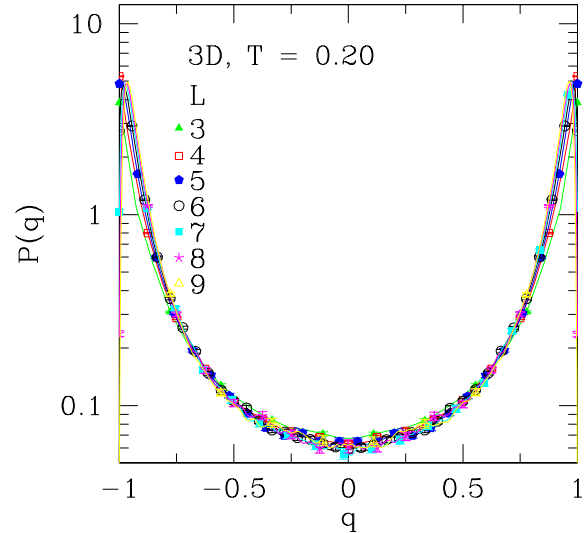


FIG. 3: Data for the overlap distribution $P(q)$ in 3D at $T = 0.20$ with free boundary conditions. Note that the vertical scale is logarithmic to better make visible both the peaks at large q and the tail down to $q = 0$. The lines go through all the data points but, for clarity, only some of the data points are shown as points.

we obtain $\theta' = 0.19 \pm 0.03$ for $T = 0.20$, $\theta' = 0.15 \pm 0.02$ for $T = 0.34$, and $\theta' = 0.05 \pm 0.02$ for $T = 0.50$. The goodness-of-fit probabilities Q for these fits²⁸ are 0.912, 0.703, and 0.384 for $T = 0.20$, 0.34, and 0.50, respectively. If we fix $\theta' = 0$, the RSB prediction, and attempt a fit to all values of L as well as a subset with $L \leq 7$ the goodness-of-fit probabilities are smaller than 10^{-6} for $T = 0.20$ and 0.34 and 0.017 for $T = 0.50$, which are rather poor. We also find that fixing $\theta' = 0$ for $L \geq 7$ is more probable than $\theta' = 0.20$.

Figures 6 and 7 show data for the link overlap q_l at $T = 0.20$ and 0.50, respectively. We see a large peak for large q_l values. The data for $T = 0.20$ show a small shoulder for smaller q_l values. This feature has been observed in Ref. 14.

Figure 8 shows data for the variance of $P(q_l)$ at several temperatures. We attempt two fits of the form

$$\text{Var}(q_l) = a + bL^{-c} \quad (5)$$

and

$$\text{Var}(q_l) = dL^{-e} \quad (6)$$

Table II shows the relevant parameters for the three-parameter fits to Eq. (5). From our data, we see a finite value of a for the sizes studied, a result that implies $d = d_s$, as expected in RSB. A two-parameter fit of the form $\text{Var}(q_l) \sim L^{-\mu}$ in Eq. (6) does not seem plausible given

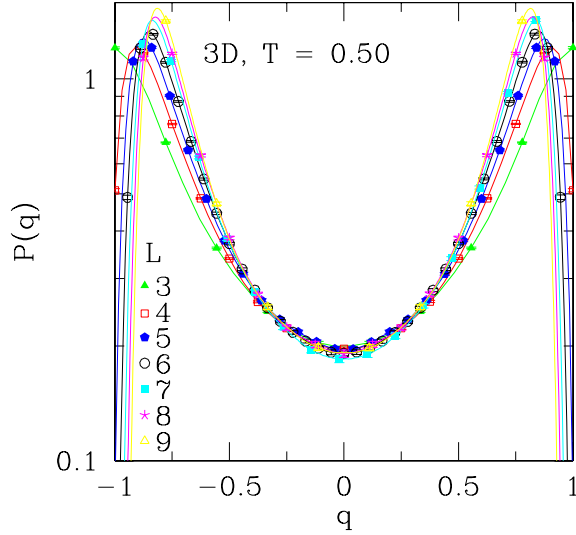


FIG. 4: Same as for Fig. 3 but at $T = 0.50$.

TABLE II: Fits for $\text{Var}(q_i)$ for the three-dimensional EA Ising spin-glass with free boundary conditions to the form in Eq. (5). We show the data for different temperatures and find a finite value for a . The fit probabilities Q are reasonable for the lower temperatures.

T	a	b	c	Q
0.20	0.0032 ± 0.0002	0.228 ± 0.006	1.860 ± 0.025	0.819
0.34	0.0027 ± 0.0003	0.349 ± 0.014	1.937 ± 0.038	0.003
0.50	0.0017 ± 0.0002	0.463 ± 0.014	2.072 ± 0.029	0.000011

the small fitting probabilities Q of 10^{-18} , 10^{-37} , and 0.0 for $T = 0.20$, 0.34 , and 0.50 , respectively. Similar results are found for zero-temperature calculations⁸.

However, given the modest range of sizes studied, and the likelihood that there are strong finite-size corrections with free boundary conditions, we cannot rule out that asymptotically one has $a = 0$, implying $d_s < d$. Evidence for large finite-size corrections with free boundary conditions comes from our estimates for T_c , which are inconsistent with known results²⁴ by $\sim 10\%$.

B. Four dimensions

Table III shows the parameters of the simulation in four dimensions. Our lowest simulated temperature is 0.20 (to be compared with $T_c \approx 1.80$)²⁹ and the largest is 2.80. We use the same temperature set for each size studied. The acceptance ratios for the parallel tempering method are typically greater than 0.3.

Figures 9 and 10 show data for $P(q)$ at temperatures

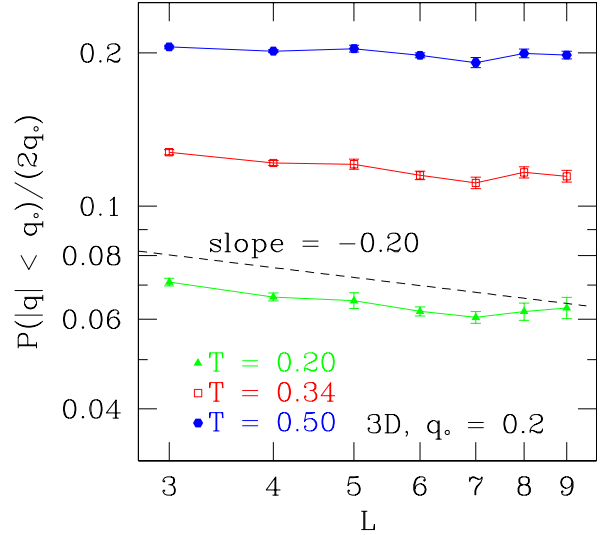


FIG. 5: Log-log plot of $P(0)$, the spin overlap at $q = 0$, against L in 3D with free boundary conditions averaged over the range $|q| < q_0 = 0.20$. The data slightly depend on system size. The dashed line has slope -0.20 , the estimated value of $-\theta$ according to the droplet picture.

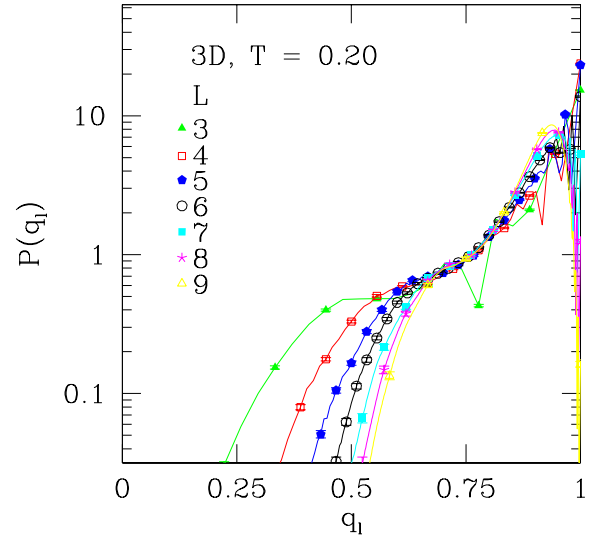


FIG. 6: The distribution of the link overlap in 3D at $T = 0.20$ with free boundary conditions for different sizes. Note the logarithmic vertical scale.

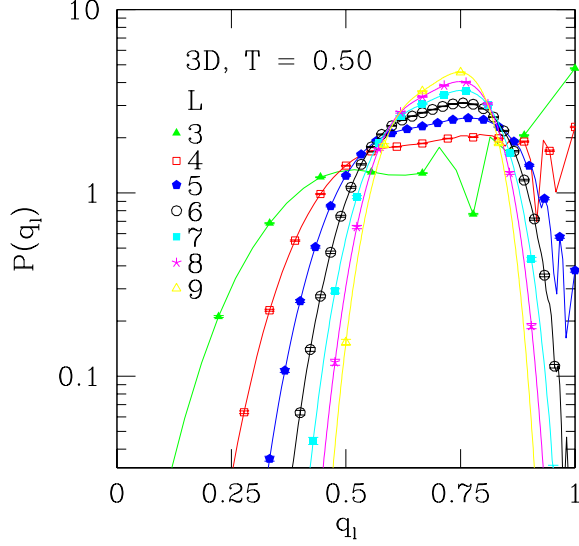


FIG. 7: Same as for Fig. 6 but at $T = 0.50$.

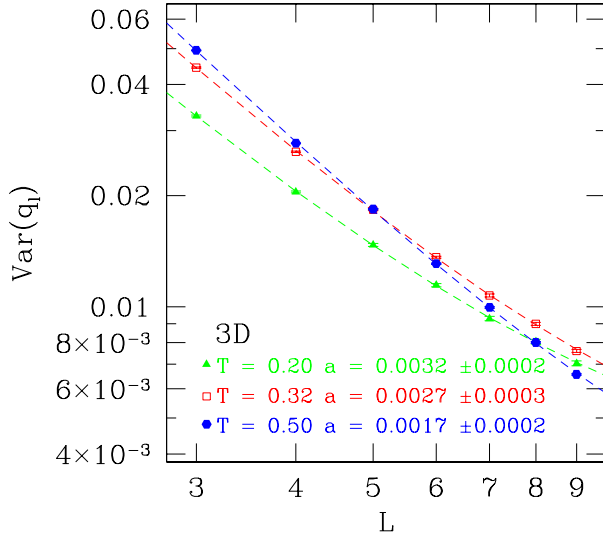


FIG. 8: Log-log plot of the variance of q_l as a function of size in 3D at several temperatures. The dashed lines correspond to fits of the form $y_l = a + bL^{-c}$.

TABLE III: Parameters of the simulations in four dimensions with free boundary conditions.

L	N_{samp}	N_{sweep}	N_T
3	10000	6×10^3	23
4	10000	6×10^4	23
5	5000	5×10^5	23

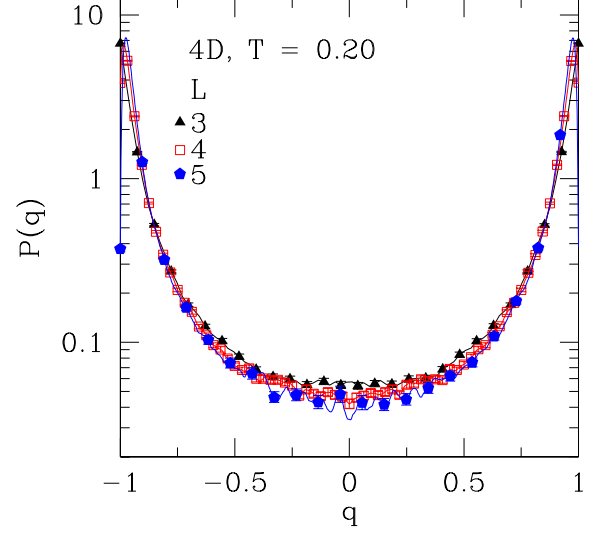


FIG. 9: Data for the overlap distribution $P(q)$ in 4D at $T = 0.20$ with free boundary conditions. The data are normalized, so the area under the curve is unity.

0.20 and 0.46. As in three dimensions, the tail of the distribution depends on the system size L . To better quantify this behavior, we show in Fig. 11 data for $P(0)$ vs L averaged over the range $|q| < 0.20$. Since the DP predicts that $P(0) \sim L^{-\theta}$, where^{30,31} $\theta \simeq 0.7$ we also indicate this behavior by the dashed line in the figure. The data is reasonably consistent with this. Fixing $\theta' = 0.70$ and performing a fit of the form $aL^{-\theta'}$, we find goodness-of-fit probabilities Q of 0.53, 0.44, and 0.21 for $T = 0.20, 0.25$, and 0.32, respectively. Fixing $\theta' = 0$ gives us goodness-of-fit probabilities $Q < 10^{-4}$. Unfortunately, our modest range of sizes does not permit us to make more quantitative statements and a crossover to a behavior where $P(0) \sim L^0$ cannot be excluded. As in three dimensions, our data is consistent with $P(0) \propto T$ for $T \rightarrow 0$.

The data for the distribution of the link overlap is shown in Figs. 12 and 13 for temperatures 0.20 and 0.46, respectively. As in three dimensions, we see a double-peak structure.

In Fig. 14 we show the variance of the link overlap q_l as a function of system size for several low temperatures. We perform fits to the functions indicated in Eqs. (5) and (6). Table IV shows the results of the three-parameter fits to Eq. (5). The best fit has $a > 0$, a result compatible with RSB, but, because we have the same number of data points as parameters, we cannot give an error bar or fit probability Q . Table V shows the results of the two-parameter fits to Eq. (6). The goodness-of-fit probabilities are quite small, but not impossibly so for small T , so we cannot rule out a scenario in which $\text{Var}(q_l) \rightarrow 0$ for $L \rightarrow \infty$.

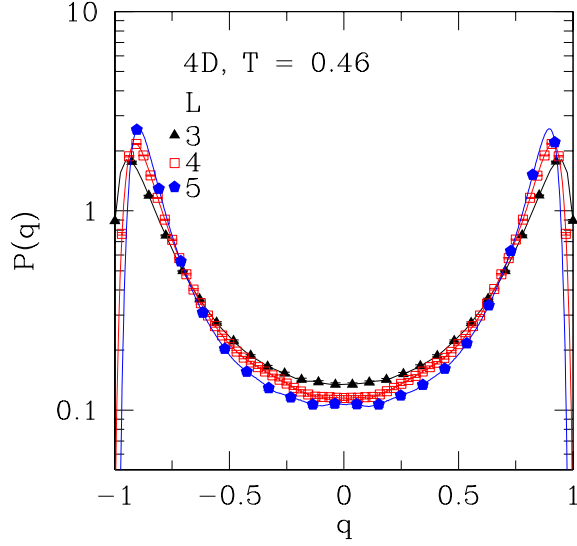


FIG. 10: Same as for Fig. 9 but at $T = 0.46$.

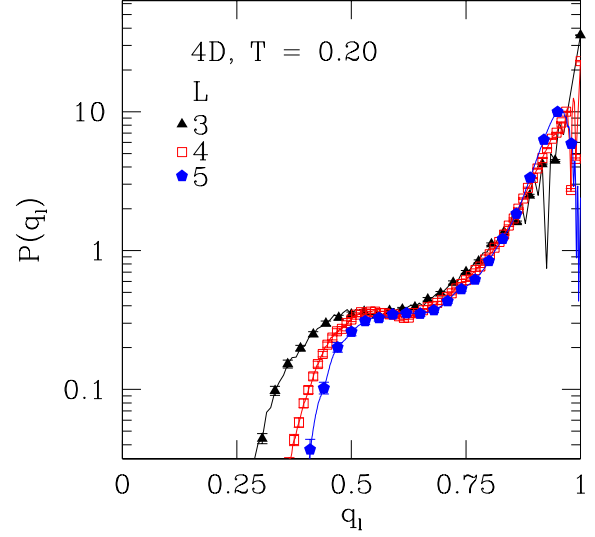


FIG. 12: The distribution of the link overlap in 4D at $T = 0.20$ for different sizes with free boundary conditions. Note the logarithmic vertical scale.

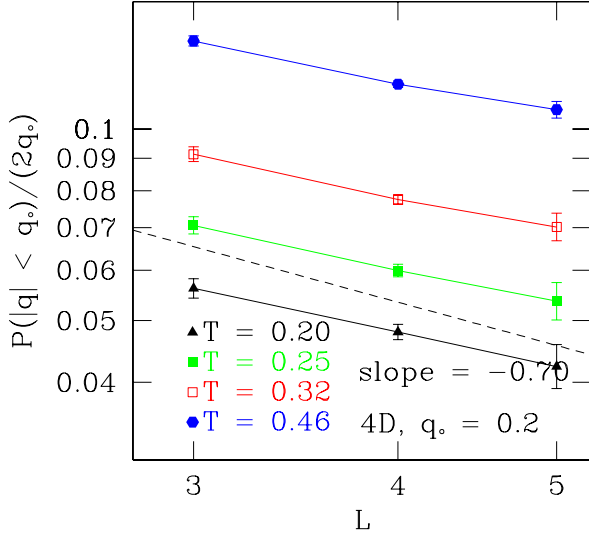


FIG. 11: Log-log plot of $P(0)$ against L in 4D averaged over the range $|q| < q_o = 0.20$. For small sizes a decrease in $P(0)$ with increasing system size is visible.

V. CONCLUSIONS

We have performed Monte Carlo simulations of the three- and four-dimensional EA Ising spin glass with free boundary conditions. For small sizes, we find $P(0) \sim L^{-\theta'}$ with $\theta' > 0$. The values of θ' we obtain for the

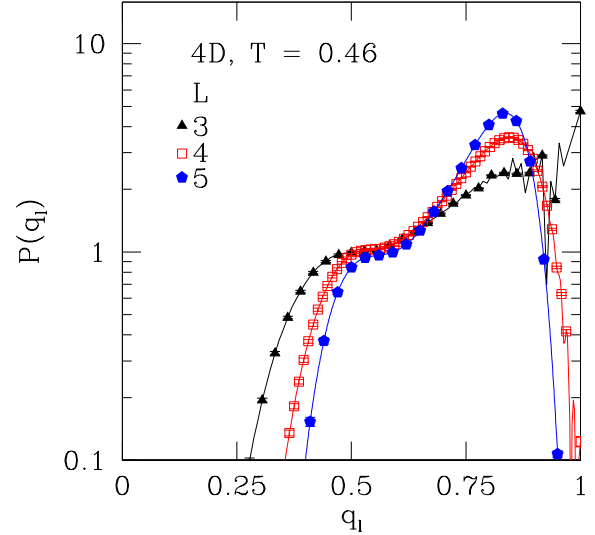


FIG. 13: Same as for Fig. 12 but at temperature 0.46.

lowest temperatures simulated are compatible with predictions from the droplet model. However, in three dimensions, we find evidence for crossover to a behavior where $P(0) \sim L^0$ for larger system sizes. In four dimensions, where the range of sizes is smaller, we do not see evidence for this crossover. An analysis of our results

TABLE IV: Fits for $\text{Var}(q_l)$ for the four-dimensional EA Ising spin glass with free boundary conditions for the fit in Eq. (5). We show the data for different temperatures and find a finite value for a . We cannot quote error bars or fitting probabilities since we have the same number of data points as variables.

T	a	b	c
0.20	0.0063	0.1517	2.0156
0.32	0.0057	0.1980	1.9342
0.46	0.0057	0.2729	2.1285

TABLE V: Fits for $\text{Var}(q_l)$ for the four-dimensional EA Ising spin glass with free boundary conditions for the fit in Eq. (6). The probabilities for the fit are quite small but not impossibly so for small T .

T	d	e	Q
0.20	0.090 ± 0.008	1.255 ± 0.005	0.09
0.32	0.137 ± 0.010	1.406 ± 0.003	0.05
0.46	0.179 ± 0.015	1.572 ± 0.002	0.0008

indicates that the surface of these excitations is space filling, corresponding to RSB. However, since free boundary conditions have large finite-size corrections, it is not clear if these results represent the asymptotic behavior. Overall, our results are quite similar to those of Ref. 8, which were obtained at zero temperature.

Although free boundary conditions have large finite-size corrections because a substantial fraction of spins

are on the surface, there is also a compensating benefit in that they do not pose any restrictions on the position of domain walls (see Fig. 1). It would be interesting to investigate what the optimal boundary conditions for spin-glass studies.

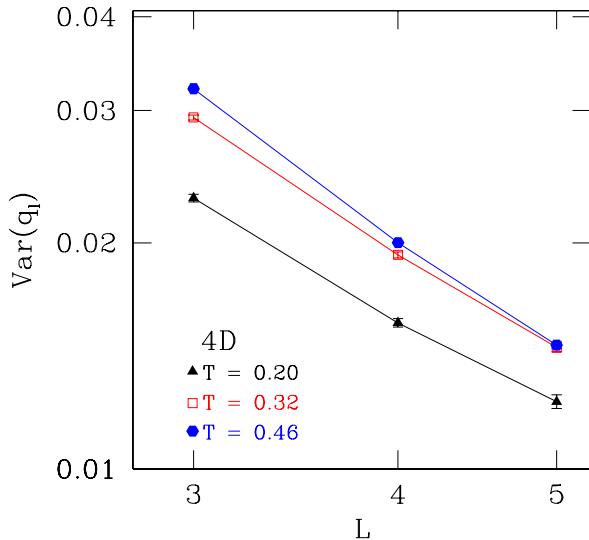


FIG. 14: Log-log plot of the variance of q_l as a function of size in 4D at several temperatures with free boundary conditions. The data do not fit well to a power law.

Acknowledgments

We would like to thank M. Palassini for useful discussions. This work was supported by the National Science Foundation under grant No. DMR 0086287. The numerical calculations were made possible by use of the UCSC Physics graduate computing cluster funded by the Department of Education Graduate Assistance in the Areas of National Need program. We also thank Gary Glatzmaier for allowing us to use the 32-node Beowulf cluster at the UCSC Earth Sciences Department, which is funded by NASA's Planetary Geology and Geophysics Program.

-
- * Electronic address: dummkopf@physics.ucsc.edu; Present address: Department of Physics, University of California, Davis, CA 95616
- † Electronic address: peter@bartok.ucsc.edu; URL: <http://bartok.ucsc.edu/peter>; Present address: Department of Theoretical Physics, 1, Keble Road, Oxford OX1 3NP, England
- ¹ M. Palassini and A. P. Young, *Triviality of the ground state structure in Ising spin glasses*, Phys. Rev. Lett. **83**, 5126 (1999), (cond-mat/9906323).
 - ² F. Krzakala and O. C. Martin, *Spin and link overlaps in 3-dimensional spin glasses*, Phys. Rev. Lett. **85**, 3013 (2000).
 - ³ M. Palassini and A. P. Young, *Nature of the spin glass state*, Phys. Rev. Lett. **85**, 3017 (2000), (cond-mat/0002134).
 - ⁴ E. Marinari and G. Parisi, *On the effects of changing the boundary conditions on the ground state of Ising spin glasses*, Phys. Rev. B **62**, 11677 (2000).
 - ⁵ E. Marinari and G. Parisi, *On the effects of a bulk perturbation on the ground state of 3d Ising spin glasses*, Phys. Rev. Lett. **86**, 3887 (2001), (cond-mat/0007493).
 - ⁶ A. A. Middleton, *Numerical investigation of the thermodynamic limit for ground states in models with quenched disorder*, Phys. Rev. Lett. **83**, 1672 (1999).
 - ⁷ A. A. Middleton, *Energetics and geometry of excitations in random systems*, Phys. Rev. B **63**, 060202(R) (2001).
 - ⁸ M. Palassini, F. Liers, M. Jünger, and A. P. Young (2001), manuscript in preparation.
 - ⁹ G. Parisi, *Infinite number of order parameters for spin-glasses*, Phys. Rev. Lett. **43**, 1754 (1979).
 - ¹⁰ M. Mézard, G. Parisi, and M. A. Virasoro, *Spin Glass Theory and Beyond* (World Scientific, Singapore, 1987).
 - ¹¹ D. S. Fisher and D. A. Huse, *Absence of many states in realistic spin glasses*, J. Phys. A **20**, L1005 (1987).
 - ¹² D. A. Huse and D. S. Fisher, *Pure states in spin glasses*, J. Phys. A **20**, L997 (1987).
 - ¹³ D. S. Fisher and D. A. Huse, *Equilibrium behavior of the spin-glass ordered phase*, Phys. Rev. B **38**, 386 (1988).
 - ¹⁴ H. G. Katzgraber, M. Palassini, and A. P. Young, *Monte Carlo simulations of spin glasses at low temperatures*, Phys. Rev. B **63**, 184422 (2001), (cond-mat/0108320).
 - ¹⁵ E. Marinari, G. Parisi, F. Ricci-Tersenghi, J. J. Ruiz-Lorenzo, and F. Zuliani, *Replica symmetry breaking in short range spin glasses: A review of the theoretical foundations and of the numerical evidence*, J. Stat. Phys. **98**, 973 (2000).
 - ¹⁶ J. D. Reger, R. N. Bhatt, and A. P. Young, *A Monte Carlo study of the order parameter distribution in the four-dimensional Ising spin glass*, Phys. Rev. Lett. **64**, 1859 (1990).
 - ¹⁷ E. Marinari, G. Parisi, and J. J. Ruiz-Lorenzo, *Numerical simulations of spin glass systems*, in *Spin Glasses and Random Fields*, edited by A. P. Young (World Scientific, Singapore, 1998), p. 59.
 - ¹⁸ E. Marinari and F. Zuliani, *Numerical simulations of the 4d Edwards-Anderson spin glass with binary couplings*, J. Phys. A **32**, 7447 (1999).
 - ¹⁹ A. J. Bray and M. A. Moore, *Scaling theory of the ordered phase of spin glasses*, in *Heidelberg Colloquium on Glassy Dynamics and Optimization*, edited by L. Van Hemmen and I. Morgenstern (Springer, New York, 1986), p. 121.
 - ²⁰ M. A. Moore, H. Bokil, and B. Drossel, *Evidence for the droplet picture of spin glasses*, Phys. Rev. Lett. **81**, 4252 (1998).
 - ²¹ H. Bokil, B. Drossel, and M. A. Moore, *Influence of critical behavior on the spin-glass phase*, Phys. Rev. B **62**, 946 (2000).
 - ²² K. Hukushima and K. Nemoto, *Exchange Monte Carlo method and application to spin glass simulations*, J. Phys. Soc. Japan **65**, 1604 (1996).
 - ²³ E. Marinari, *Optimized Monte Carlo methods*, in *Advances in Computer Simulation*, edited by J. Kertész and I. Kondor (Springer Verlag, Berlin, 1998), p. 50, (cond-mat/9612010).
 - ²⁴ E. Marinari, G. Parisi, and J. J. Ruiz-Lorenzo, *On the phase structure of the 3d Edwards Anderson spin glass*, Phys. Rev. B **58**, 14852 (1998).
 - ²⁵ A. K. Hartmann, *Scaling of stiffness energy for three-dimensional $\pm J$ Ising spin glasses*, Phys. Rev. E **59**, 84 (1999).
 - ²⁶ A. J. Bray and M. A. Moore, *Lower critical dimension of Ising spin glasses: a numerical study*, J. Phys. C **17**, L463 (1984).
 - ²⁷ W. L. McMillan, *Domain-wall renormalization-group study of the three-dimensional random Ising model*, Phys. Rev. B **30**, 476 (1984).
 - ²⁸ W. H. Press, S. A. Teukolsky, W. T. Vetterling, and B. P. Flannery, *Numerical Recipes in C* (Cambridge University Press, Cambridge, 1995).
 - ²⁹ G. Parisi, F. Ricci-Tersenghi, and J. J. Ruiz-Lorenzo, *Equilibrium and off-equilibrium simulations of the 4d Gaussian spin glass*, J. Phys. A **29**, 7943 (1996).
 - ³⁰ A. K. Hartmann, *Calculation of ground states of four-dimensional $\pm J$ Ising spin glasses*, Phys. Rev. E **60**, 5135 (1999).
 - ³¹ K. Hukushima, *Domain-wall free energy of spin-glass models: Numerical method and boundary conditions*, Phys. Rev. E **60**, 3606 (1999).